Bounding the minimal 331 model through the decay $B \to X_s\gamma$

Christoph Promberger,[1] Sebastian Schatt,[1] Felix Schwab,[2] and Selma Uhlig[1]

[1]*Physik Department, Technische Universität München, D-85748 Garching, Germany*
[2]*Departament de Física Teòrica, IFAE, UAB, E-08193 Bellaterra, Barcelona, Spain*

We study the decay $B \to X_s\gamma$ within the framework of the minimal 331 model, taking into account both new experimental and theoretical developments that allow us to update and improve on an existing 10 yr old analysis. In contrast to several other flavor changing observables that are modified already at tree level from a new Z' gauge boson, we have only one loop contributions in this case. Nevertheless, these are interesting, as they may be enhanced and can shed light on the charged gauge boson and Higgs sector of the model. Numerically, we find that the Higgs sector, which is well approximated by a 2 Higgs doublet model (2HDM), dominates, since the gauge contributions are already very strongly constrained. With respect to $B \to X_s\gamma$, the signal of the minimal 331 model is therefore nearly identical to the 2HDM one, which allows us to obtain a lower bound on the charged Higgs mass. Further, we observe, in analogy to the 2HDM model, that the branching fraction can be rather strongly increased for small values of $\tan\beta$. Also, we find that $B \to X_s\gamma$ has no impact on the bounds obtained on rare K and B decays in an earlier analysis.

I. INTRODUCTION

Presently, all phenomena observed in nature (with the exception of gravity) are described within the standard model (SM) of particle physics. This model seems to work beautifully up to scales of at least $\mathcal{O}(\text{TeV})$. On the other hand, successful as the SM may be, the general hope (and belief) of particle physicists is that it should be a part of a more fundamental theory. This belief is based on several theoretical shortcomings of the model, the most important of which are the instability of the Higgs mass as well as the general particle content of the model, such as the fact that each fermion type appears in three generations. This last point is addressed in the context of 331 models [1,2], where the requirement of anomaly cancellation combined with the asymptotic freedom of QCD force the number of generations to be exactly three. To achieve this, the electroweak $SU(2)_L$ of the SM is extended to an $SU(3)_L$, where the third generation is treated differently, i.e. is transformed as an antitriplet.

This setup leads to the existence of several new particles, in particular, of new gauge bosons, such as a Z' that transmits flavor changes at tree level due to the different treatment of the third generation. As a consequence, this gives rise to tree level contributions for several observables that proceed at loop level only in the SM and which have been extensively studied in the literature [3–7]. In addition to these observables, it is also interesting to investigate the inclusive decay $B \to X_s\gamma$, where X_s denotes a sum over all final states containing a strange quark. While tree level contributions are absent here, those at one loop may be interesting, and have first been studied for the minimal model (to which we will also restrict ourselves) in [8], after similar, analogous effects to ε'/ε have been investigated in [9]. There are several reasons that make this analysis worthwhile, in spite of the fact that a first reasoning would suggest to focus on tree level Z' exchange only. These are:

(i) The mechanism that causes FCNCs at tree level (i.e. the different treatment of the third generation) also enhances the one loop contribution rather strongly. This is due to the breakdown of the GIM mechanism, which acts very effectively in the SM. In any case, it was found in [8] that the new contributions could, in principle, be almost comparable in size to the SM. Since the one loop effects are also governed by other particles than the tree level ones, i.e. charged gauge bosons and Higgs fields, one may also hope to shed some light on an entirely different sector of the model.

(ii) In the ten years since the analysis of [8], the data on $B \to X_s\gamma$ have improved considerably [10–12], leading to a very precise experimental number. This can be used to place constraints on the parameter space of the model which can be compared with those coming from other FCNC processes, obtained, for example, in [6].

In view of this, we update the $B \to X_s\gamma$ analysis of [8] using new data, retaining the general scheme of that analysis. This concerns, in particular, the treatment of the QCD corrections via the renormalization group equations, and the treatment of the Higgs sector. Here, we study only an effective 2 Higgs doublet model (2HDM) type II, which is a good approximation in the flavor sector [3,8]. This analysis extends and concludes our study of FCNC processes begun in [6]. Our paper is then organized as follows: First, in Sec. II, we introduce very briefly the minimal 331 model, focusing on those parts of the model that are important for the penguin diagrams contributing. Next,

we give the most general background on $B \to X_s \gamma$ in Sec. III, where we also list and explain the different contributions to the decay and discuss the cancellation of divergences. Section IV then contains all our numerics, where we compare these new constraints with those from the measurement of the B_s^0 mass difference ΔM_s. These are the only relevant ones in this context, since the different sectors of flavor transitions sd, bd, and bs decouple. Finally, we conclude in Sec. V.

II. THE MINIMAL 331 MODEL

The minimal 331 model has been discussed extensively in [3,13,14] and in short in [6], from where we take the conventions. Many variations of this minimal model have been developed, such as ones with right-handed neutrinos, supersymmetric versions, and others [15–28]. Generally, in 331 models the electroweak $SU(2)_L$ of the SM is extended to a $SU(3)_L$, which is broken down in two steps:

$$SU(3)_C \times SU(3)_L \times U(1)_X \overset{v_\sigma}{\Rightarrow} SU(3)_C \times SU(2)_L \times U(1)_Y$$
$$\overset{v_\eta, v_\rho}{\Rightarrow} SU(3)_C \times U(1)_{em}. \quad (1)$$

Evidently, this breaking process involves three Higgs doublets, one of which develops a vacuum expectation value (VEV) at a high scale, while the other two VEVs are of the order of the weak scale. This leads to a much richer scalar sector than in the SM, which has been extensively studied for the minimal model in [29,30], as well as a more complicated Yukawa structure [3,4,13,14,19]. Physically, after absorbing the appropriate number of Goldstone bosons, one is left with one light neutral Higgs scalar, 7 heavier neutral Higgs particles as well as 4 singly and 3 doubly charged Higgs particles, all of which are heavy. On the other hand, the quark doublets of the SM are extended to triplets by adding an additional heavy quark. All of the quarks, as well as their right-handed counterparts, have three quantum numbers called X, T_3 and T_8, corresponding to the diagonal generators of $SU(3)$.

From these, the electric charge can be obtained by

$$Q = T_3 + \beta T_8 + X; \qquad \beta = \sqrt{3} \quad (2)$$

in our normalization of the hypercharge X. To ensure anomaly cancellation, the third generation couples differently than the first two. This has the important consequence of generating flavor changing neutral currents at tree level. Another curiosity of the minimal 331 model is the Landau Pole that can arise at rather low energies. It becomes apparent when one expresses the ratio of $SU(3)$ and $SU(2)$ couplings through the Weinberg angle as

$$\frac{g_X^2}{g^2} = \frac{6\sin^2\theta_W}{1-4\sin^2\theta_W}. \quad (3)$$

Clearly, the theory is ill defined if $\sin^2\theta_W$ grows to be $1/4$, which puts an upper limit on the scale of the symmetry

breaking as well as on the heavy gauge boson masses. Analyzing this carefully [31], gives an upper bound of several TeV for the Z' mass, so that in the numerical analysis below we will follow [6] and use values of up to $M_{Z'} = 5$ TeV. In choosing $\beta = \sqrt{3}$ in (2), and assigning the appropriate hypercharge structure, we have distinguished the model to be the *minimal* 331 model.

Turning now to the gauge boson content, one finds that the breaking process sketched above produces, in addition to the SM gauge bosons, an additional neutral Z' boson as well as singly charged $Y^\pm$ and doubly charged $Y^{\pm\pm}$ bosons. The photon is massless, as required, since a $U(1)$ remains unbroken while the W and Z masses are at the weak scale, as required. Finally, all additional gauge bosons obtain their masses from the large VEV v_σ and are therefore heavier. Assuming that this heavy VEV is much larger than the others, an interesting relation between the heavy gauge boson masses can be found, which allows to express the $Y^\pm$ mass in terms of the Z' mass or vice versa:

$$M_{Y^\pm}^2 = \frac{3}{4} \frac{(1 - 4\sin^2\theta_W)}{(\cos^2\theta_W)} M_{Z'}^2, \quad (4)$$

while $M_{Y^\pm} = M_{Y^{\pm\pm}}$. We will be more explicitly concerned with the respective fermion couplings below, but let us already here state that in the quark sector the new charged gauge bosons always transmit a coupling from a SM light quark to an additional heavy one, and therefore do not modify the amplitudes of low energy observables at tree level.[1] The neutral Z', on the other hand, also has couplings to light quarks only, and does give this kind of contributions. In the decay $B \to X_s \gamma$, however, both charged and neutral gauge bosons are equally important, so that information on the charged bosons may be obtained.

After these more general remarks, let us now show explicitly the respective fermion couplings. Concerning the neutral currents, the Lagrangian for the above-mentioned FCNCs at tree level is given by

$$\mathcal{L}_{\text{FCNC}} = \frac{gc_W}{\sqrt{3}\sqrt{1-4s_W^2}} \left[\bar{u}\gamma_\mu\gamma_L U_L^\dagger \begin{pmatrix} 0 & & \\ & 0 & \\ & & 1 \end{pmatrix} U_L u \right.$$
$$\left. + \bar{d}\gamma_\mu\gamma_L \tilde{V}_L^\dagger \begin{pmatrix} 0 & & \\ & 0 & \\ & & 1 \end{pmatrix} \tilde{V}_L d \right] Z'^\mu. \quad (5)$$

The explicit couplings to fermions and a possible parametrization for the new mixing matrices U_L and $\tilde{V}_L$, that diagonalize the up and down-type Yukawa couplings, respectively, have been given in [6]. These obey

---

[1]This is no longer true in the lepton sector, where, for example, a new tree level diagram to muon decay modifies the Fermi coupling constant [6].
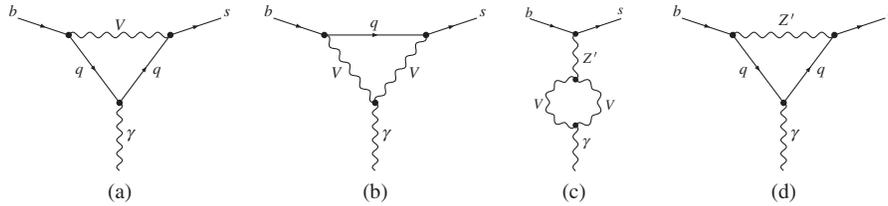
FIG. 1.   New magnetic penguin diagrams contributing to the decay $B \to X_s \gamma$. V denotes the heavy charged gauge bosons $Y^\pm$, $Y^{\pm\pm}$. We do not show self-energies and the diagrams involving Goldstone bosons.

$$U_L^\dagger \tilde{V}_L = V_{\text{CKM}}, \qquad (6)$$

and the notation of (5) and (6) is to be understood as in [6], so that the tilde distinguishes between the SM CKM matrix V_{CKM} and the mixing matrix for the down-type quarks.

Additionally, the charged current vertices in this basis are then

$$J_{W^+}^\mu = \bar{u}\gamma^\mu \gamma_L U_L^\dagger \tilde{V} d = \bar{u}\gamma^\mu \gamma_L V_{\text{CKM}} d$$

$$J_{Y^+}^\mu = \bar{d}\gamma^\mu \gamma_L \tilde{V}^\dagger \begin{pmatrix} 1 & 0 \\ 0 & 1 \\ 0 & 0 \end{pmatrix} D + \bar{T}\gamma^\mu \gamma_L (0 \quad 0 \quad 1) U_L u$$

$$J_{Y^{++}}^\mu = \bar{u}\gamma^\mu \gamma_L U_L^\dagger \begin{pmatrix} 1 & 0 \\ 0 & 1 \\ 0 & 0 \end{pmatrix} D - \bar{T}\gamma^\mu \gamma_L (0 \quad 0 \quad 1) \tilde{V} d.$$

$$(7)$$

From these equations, it becomes obvious that there can be new penguin diagrams in the decay $B \to X_s \gamma$ containing heavy quarks and heavy gauge bosons in the loop. We will discuss the result for these diagrams, shown in Fig. 1, along with all other new contributions in the next section. Concerning the notation, here and in the following we denote by V the heavy charged gauge bosons.

In the Higgs sector the symmetry breaking structure leads to a number of charged and neutral Higgs fields, which in principle also transmit flavor changing interactions. Considering the heavy top quark coupling only, the quark sector can be identified with a modified 2 Higgs doublet model (2HDM) type II, in which only the third generation diagrams are taken into account.[2] This corresponds to [8], where the Higgs sector has been approximated in this way. This approximation also assumes that the additional charged Higgs from the sextet, coupling only to leptons, does not mix with the one from the triplet, which corresponds to the one that exists in the 2HDM. Note that these kind of terms do not appear in FCNC processes mediated by a tree level Z', since there the top Yukawa does not appear. However, for $B \to X_s \gamma$ they should be added.

---

[2]Note also that due to the exchange of the top and bottom quark in the third quark triplet, the couplings are accordingly exchanged.

III. PRESENT SITUATION OF THE DECAY $B \to X_s \gamma$

We begin with several general remarks concerning the decay $B \to X_s \gamma$, while the interested reader may consult [32] for a very recent and more elaborate discussion of the theoretical and experimental background. In general, theoretical interest in this decay stems from the following features:

  (i) Being an inclusive process, it can be calculated much more reliably than exclusive processes generally can be. Using the heavy quark expansion, the calculation can be performed at the partonic level, while additional corrections are suppressed by terms of $\mathcal{O}(1/m_b)$.

  (ii) The decay is by now very precisely measured. In addition to the increasingly precise SM calculation, it therefore offers a very good test of the SM or a nice tool to search for physics beyond it.

Theoretically the decay $B \to X_s \gamma$ has now been calculated completely up to NLL precision, and recently a first estimate of the value at NNLL precision has been obtained [33], after a great effort of many groups to calculate the different contributions required [34]. It reads:

$$\text{Br}(B \to X_s \gamma)|_{\text{NNLL}} = (3.15 \pm 0.23) \times 10^{-4}. \qquad (8)$$

This effort of the NNLL calculation had become necessary, due to a large uncertainty of the NLL calculation resulting from uncertainties in the charm mass renormalization scheme and scale.

On the other hand, the current experimental average is combined from the measurements of *BABAR*, Belle, CLEO, and others, using inclusive and exclusive methods. Using a photon energy cut of $E_\gamma > 1.6$, HFAG gives an average of [35]

$$\text{Br}(B \to X_s \gamma)|_{\text{Exp}} = (3.55 \pm 0.24^{+0.09}_{-0.10} \pm 0.03) \times 10^{-4},$$

$$(9)$$

where the errors include also those from the extrapolation to lower energies. Therefore, the experimental value is somewhat higher than the theoretical one, but still quite well compatible.

Let us also note here that the decay $B \to X_s \gamma$ has been analyzed in various models beyond the SM, among these

the 2HDM type II [36], the general as well as the minimal flavor violating (MFV) minimal supersymmetric SM (MSSM) [37], models with one [38] or two [39] universal extra dimensions (UED) and the littlest Higgs model with [40] and without [41] T parity. Some of these analyses have been performed at the NLO level, but most of them are done at LO order only. A comparison and compilation of the main results can be found in [32].

A. New contributions to $B \rightarrow X_s \gamma$ in the minimal 331 model

In this section, we list all the different contributions to the decay $B \rightarrow X_s \gamma$ that modify the prediction of the 331 model with respect to the SM, and comment briefly on the cancellation of divergences. All expressions are explicitly given in [8]. Concentrating on the operators that are relevant for $B \rightarrow X_s \gamma$, we have also confirmed the calculation of [8].

There are three different possibilities for the additional particles to show up in the decay $B \rightarrow X_s \gamma$. First of all, there are penguin diagrams involving the new charged gauge bosons, shown in the first two diagrams of Fig. 1. For an arbitrary charged gauge boson and quark, the general structure, after calculating all penguin and the self energy diagrams required and summing over all of these, is a well known generalization of the Inami Lim Functions. In this calculation, a divergent term remains, which additionally violates gauge invariance. Within the SM, this term is canceled by the GIM mechanism when summing over all quark flavors. In the 331 model, this singularity is not removed entirely even then, due to the different charge assignment of the quarks. In this case, the cancellation is achieved [8,9] by adding the $Z' - \gamma$ mixing diagram shown in Fig. 1(c). Therefore, the very same mechanism that generated the FCNCs at tree level can potentially also enhance them at loop level, in particular, if the GIM mechanism is as effective in the SM as it is in $B \rightarrow X_s \gamma$.

Next, there are also the Z' penguin diagrams shown in Fig. 1(d). To simplify the expressions, we assume that all quark masses vanish (in this case, there are down-type quarks also in the loop). The unitarity of the mixing matrix $\tilde{V}$ then allows to sum up the terms from the d, c, and b quarks into a simple form without any leftover divergence.

Finally, there are contributions from the Higgs sector of the model. Calculating these explicitly results in extremely complicated expressions, due to the elaborate structure of the Higgs mass terms. Resorting to the simplifications mentioned above, one can describe the Higgs sector by the 2HDM, where the corresponding expressions are well known [36].

B. Initial conditions and renormalization group analysis

The standard procedure of calculating any weak decay is the framework of a weak effective Hamiltonian. Here, the separation of scales is achieved by integrating out all heavy degrees of freedom, and casting the Hamiltonian into an effective form:

$$\mathcal{H}_{\text{eff}} = -2\sqrt{2}G_F \sum_i C_i(\mu)O_i(\mu). \tag{10}$$

The sum extends over all operators that can appear at a given scale. Within the SM, the masses of the heavy particles are all of the order of the weak scale, at which initial conditions are then calculated. Next, the QCD corrections arising from the renormalization group running further enhance the branching fraction of $B \rightarrow X_s \gamma$ by about a factor of 3, due to the effectiveness of the GIM suppression in this case. Within the 331 model, the QCD corrections are not expected to be as important [8], but we take them into account for completeness. We use the leading order formulae for the RG running, with the anomalous dimensions as given in [8], where they have been extended from the SM to include the additional operators present in the 331 case. Turning to the matching conditions in the 331 model, there are evidently now additional scales in the problem. In principle, there is the scale of the Z' boson mass, as well as that of the masses of the charged gauge bosons. The QCD running between these two scales does not modify the values of the coefficients by much, and we therefore integrate out all heavy particles at the lower scale M_Y. These are, in addition to the heavy gauge bosons, also the heavy quarks, while the Higgs sector is added at lower energies.

These initial conditions are run down to the weak scale, where several changes occur: First, the top quark is integrated out, and along with it the operators in which the top quark appears. These are replaced by the standard operators $Q_{1/2}$ involving the charm quark. Next, we should here add the SM matching conditions as well as those from the 2HDM.

Finally, from these coefficients, the branching ratio of $B \rightarrow X_s \gamma$ is calculated by

$$\frac{\Gamma(b \rightarrow s\gamma)}{\Gamma(b \rightarrow ce\bar{\nu}_e)} = \frac{|V_{ts}^* V_{tb}|^2}{|V_{cb}|^2} \frac{6\alpha}{\pi C}(|C_7(\mu_b)|^2 + N(E_0)),$$

$$\tag{11}$$

in the notation of [42], where $C = |V_{ub}/V_{cb}|^2 \Gamma(b \rightarrow ce\bar{\nu}_e)/\Gamma(b \rightarrow ue\bar{\nu}_e) = 0.58 \pm 0.016$ and $N(E_0) = 0.0031$ are the nonperturbative corrections (we take Br$(b \rightarrow ce\bar{\nu}_e) = 0.106$). Using the SM expression for C_7 given above leads to the LO value of the branching fraction, which, numerically, does not agree with the most recent theoretical value given in [33]. To accommodate for the corresponding shift, we directly set the SM part of C_7 to the NNLO value and go through the entire RGE procedure only for the new physics contributions.

VI. NUMERICAL ANALYSIS

A. Preliminaries

We will now analyze numerically the new contributions to the decay $B \rightarrow X_s \gamma$ and investigate whether additional bounds on the minimal 331 model can be obtained from this mode and which of the parameters appearing have the strongest influence.

As constraints we will use the existing data from K and B meson mixing, such as $\Delta M_{d/s}$, $\sin 2\beta$, ΔM_K and ε_K whose theoretical expressions in the 331 model are given in [6]. As numerical input we will take the tree level values of $|V_{us}|$, $|V_{ub}|$, $|V_{cb}|$ given in [6], and $\gamma = (82 \pm 20)°$. Further, we follow the analysis of [40] and set all non-perturbative parameters to their central values and allow ΔM_K, ε_K, ΔM_d, and ΔM_s to differ from their experimental values by $\pm 50\%$, $\pm 40\%$, $\pm 40\%$ and $\pm 40\%$ respectively. In the case of $\Delta M_s / \Delta M_d$ we will choose $\pm 20\%$ as the error on the relevant parameter ξ is smaller than in the case of ΔM_d and ΔM_s separately. Similarly, we will absorb the SM uncertainties of $B \rightarrow X_s \gamma$, stemming mainly from the remaining scale uncertainty in the charm mass as well as the CKM factors, into the experimental uncertainty by increasing it to $\pm 15\%$ instead of the $\pm 8\%$ given above.

We then perform a scan over the parameters of the 331 model considering the following ranges:

$$m_T, m_S = 250\text{--}1000 \text{ GeV}, \qquad M_{H^+} = 300\text{--}2000 \text{ GeV},$$

$$M_{Z'} = 1000\text{--}5000 \text{ GeV}.$$

The three angles and the three phases of the new mixing matrix $\tilde{V}$ are kept arbitrary. Further, the expressions for the 2HDM depend on $\tan\beta$, which we mainly restrict to values of $\tan\beta > 1$ for reasons that will become evident during our analysis. We observe that, in a parametrization of the $\tilde{V}$ matrix that keeps the real and imaginary parts of the relevant combinations of $V_{ij}^* V_{lm}$ as independent, the only bound we need to consider will be the one coming from ΔM_s.

B. Constraints from $B \rightarrow X_s \gamma$ compared to other constraints

Let us first elaborate on the influence of the chosen values for $\tan\beta$. Looking at Fig. 2, we observe that the value obtained for $B \rightarrow X_s \gamma$ is practically independent of its numerical value as long as $\tan\beta > 2$. On the other hand, large values of the branching fraction can be obtained for smaller values of $\tan\beta$. This effect of the 2HDM is well known [36], and has most recently been investigated and numerically updated in [33]. We refer the reader to the detailed discussion of $B \rightarrow X_s \gamma$ within the 2HDM given there, and in the following fix $\tan\beta = 2$, in order to show more clearly the additional effects of the 331 model. In this context, we would like to point out that, in the pure 2HDM, very small values of $\tan\beta$ are excluded by other observ-
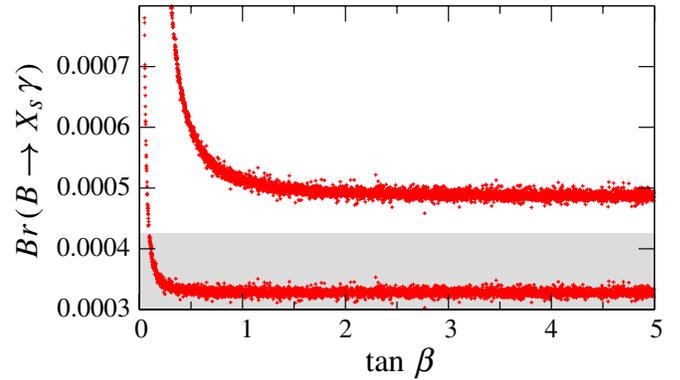
FIG. 2 (color online). The dependence of $\text{Br}(B \rightarrow X_s \gamma)$ on $\tan\beta$. For values of $\tan\beta$ below 0.5 significant enhancements are possible. The gray band indicates $\text{Br}(B \rightarrow X_s \gamma)|_{\text{Exp}}$, with errors inflated as described in the text. The upper band shows the values for $M_{H^+} = 300$ GeV, while the lower one shows those for $M_{H^+} = 5000$ GeV

ables, such as electroweak precision tests. While the 331 model does no longer resemble the 2HDM when gauge bosons are included, we use only the larger values for $\tan\beta$.

Next, we show in Fig. 3 the dependence of the branching fraction on the Z' mass, where we separate the dependence on the charged Higgs mass by showing only the values obtained for the upper and lower bound on M_{H^+}, respectively. In any case, the upper line corresponds to the lower value of M_{H^+}, meaning that the branching fraction increases with decreasing Higgs mass. The width of the remaining bands corresponds then to the allowed range of $V_{32}^* V_{33}$ and the heavy quark masses. Clearly, a variation in the charged Higgs mass has a much stronger influence on the value of the branching fraction, which leads us to conclude that, as a whole, the 2HDM contributions vastly dominate over those from the gauge bosons, and that, therefore, the signature of the minimal 331 model with respect to $B \rightarrow X_s \gamma$ is basically identical. On the other
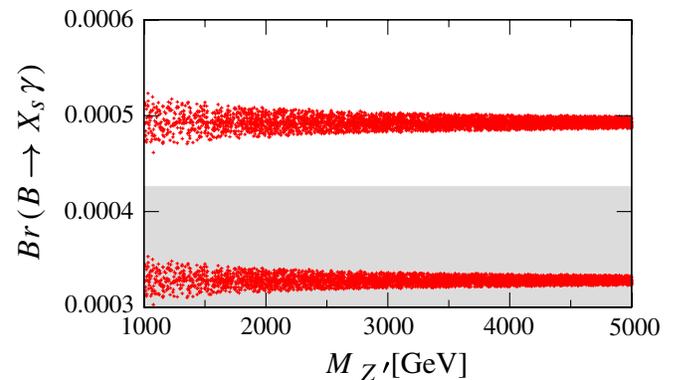
FIG. 3 (color online). $\text{Br}(B \rightarrow X_s \gamma)$ versus $M_{Z'}$. The gray band shows the experimental range with a 15% error. The upper band corresponds to a Higgs mass of $M_{H^+} = 300$ GeV and the lower one to $M_{H^+} = 2000$ GeV.
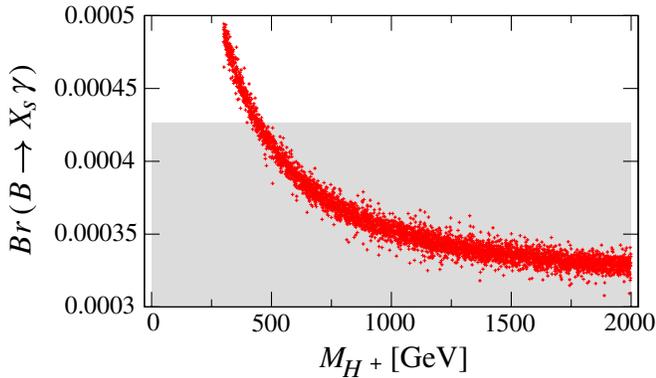
FIG. 4 (color online). $\mathrm{Br}(B \to X_s \gamma)$ versus M_{H^+}. The gray band shows the experimental range with a 15% error. From the plot one finds a lower bound on the charged Higgs mass of roughly 400 GeV.

FIG. 5 (color online). Correlation of $B \to X_s \gamma$ with the deviation of $\mathrm{Br}(B_s) \equiv \mathrm{Br}(B_s \to \mu^+ \mu^-)$ from the SM. The experimental range of the former (given by gray band) does not further constrain the range of the latter.

hand, the bounds on the Higgs sector from the type II 2HDM can immediately be applied to the 331 model. Also, we can conclude that the decay $B \to X_s \gamma$ would be well suited to explore the Higgs sector of the 331 model without additional pollution from gauge bosons, if the minimal 331 model should be established through other channels. These results represent the main conclusions of our analysis.

In this context, we also show the corresponding dependence of the branching fraction on the charged Higgs mass M_{H^+} in Fig. 4, which in principle allows us to read off a lower bound for $M_{H^+} \approx 400$ GeV. One should now take into account the NLO corrections within the SM and the 2HDM, which are known to be significant, in order to improve quantitatively on this bound. However, since $B \to X_s \gamma$ has been studied elaborately, both in the SM and the 2HDM, in [33], including every known contributions to this decay, we consider it beyond the scope of our paper to repeat this analysis and simply quote the lower bound of the Higgs mass as

$$M_{H^+} \geq 295 \text{ GeV} \qquad (95\% \text{ C.L.}). \qquad (12)$$

Interestingly, while the 331 model can, in principle, either enhance or suppress the branching fraction of $B \to X_s \gamma$, depending on the sign of the mixing matrix elements, the model as a whole predicts an enhancement of the branching fraction, due to this strong dominance of the 2HDM model. This is, of course, rather fortunate considering the present experimental result. Finally, let us comment on the modifications that we expect if we include the charged Higgs mixing that we have neglected up to now. Numerically, this introduces an additional mixing angle, as well as the corresponding modifications in the 2HDM terms. Barring some fine tuning in these expressions, this should not affect our main statement that the Higgs sector gives the main contribution to $B \to X_s \gamma$.

We will close this subsection and our numerical analysis with some very brief remarks concerning the possible
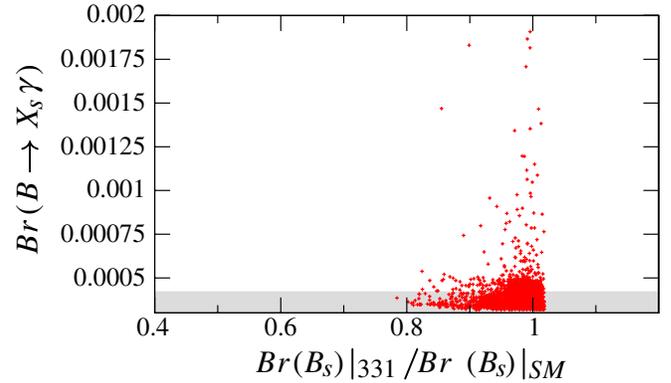
influence on the rare decays and the other observables discussed in [6]. However, after the findings of the last paragraph, one expects this influence to be completely negligible. In any case, the most interesting observable is the $B_s - \bar{B}_s$ mixing phase, which can be large. This statement is not altered by our analysis of $B \to X_s \gamma$. More interestingly, a first measurement of this quantity has recently appeared [43], which now offers some hint as to its size. As of now, this measurement is not precise enough to warrant a more detailed discussion, but it will be extremely interesting to follow the progress of the corresponding experiments.

All other statements of [6] remain unaffected, in particular, one can still obtain sizeable effects in the rare K decays, while large effects in $B_{d/s} \to \mu^+ \mu^-$ seem excluded. To show this graphically, we show in Fig. 5 the correlation between the branching fraction of $B \to X_s \gamma$ with the ratio $\mathrm{Br}(B_s \to \mu^+ \mu^-)|_{331}/\mathrm{Br}(B_s \to \mu^+ \mu^-)|_{\mathrm{SM}}$, where we observe that the gray band, representing the experimental range of $\mathrm{Br}(B \to X_s \gamma)$, still allows for the entire range of $\mathrm{Br}(B_s \to \mu^+ \mu^-)$.

V. CONCLUSIONS

Using new data for both the decay $B \to X_s \gamma$ as well as for the other existing constraints available, and in view of recent theoretical progress, including a first NNLO estimate, we have reinvestigated the implications of the minimal 331 model for the decay $B \to X_s \gamma$. In contrast to several other FCNC observables, that are affected at tree level by Z' contributions within this model, we are dealing here with a purely loop induced process, which, due to the breaking of the GIM mechanism, may still receive significant contributions. We have in general retained the general feature of the more than 10 yr old analysis performed in [8], which particularly concerns the performed simplifications within the Higgs sector. It is described here in terms of an effective 2HDM, so that the new contributions to the

branching fraction can be discussed in terms of two different parts: one originating from the extended Higgs sector and the other one from the additional gauge bosons and quarks. The latter are governed by the new mixing matrix $\tilde{V}$, that appears as a set of new parameters in the model, and is constrained by the existing bounds from FCNC processes. On the other hand, the 2HDM contribution is only constrained by the usual parameter constraints on the Higgs mass. The main new result of our analysis is the finding that the gauge contributions are now constrained so strongly that effectively one is left with the 2HDM ones. Thus, it is possible to obtain a lower bound on the charged Higgs mass, as obtained from a recent, more sophisticated analysis of the 2HDM. We therefore conclude that the decay $B \rightarrow X_s \gamma$ is a very useful tool to probe the Higgs sector of the minimal 331 model and is therefore complementary to other FCNC observables. This shows once again the power of the B and K meson systems in obtaining information about models beyond the SM, when they are used together and combined.

[1] P. H. Frampton, Phys. Rev. Lett. **69**, 2889 (1992).
[2] F. Pisano and V. Pleitez, Phys. Rev. D **46**, 410 (1992); R. Foot, O. F. Hernandez, F. Pisano, and V. Pleitez, Phys. Rev. D **47**, 4158 (1993).
[3] J. T. Liu and D. Ng, Phys. Rev. D **50**, 548 (1994).
[4] D. Gomez Dumm, F. Pisano, and V. Pleitez, Mod. Phys. Lett. A **9**, 1609 (1994).
[5] J. A. Rodriguez and M. Sher, Phys. Rev. D **70**, 117702 (2004).
[6] C. Promberger, S. Schatt, and F. Schwab, Phys. Rev. D **75**, 115007 (2007).
[7] R. Martinez and F. Ochoa, Phys. Rev. D **77**, 065012 (2008).
[8] J. Agrawal, P. H. Frampton, and J. T. Liu, Int. J. Mod. Phys. A **11**, 2263 (1996).
[9] J. Agrawal and P. H. Frampton, Nucl. Phys. **B419**, 254 (1994).
[10] P. Koppenburg *et al.* (Belle Collaboration), Phys. Rev. Lett. **93**, 061803 (2004).
[11] B. Aubert *et al.* (*BABAR* Collaboration), Phys. Rev. D **72**, 052004 (2005).
[12] B. Aubert *et al.* (*BABAR* Collaboration), Phys. Rev. Lett. **97**, 171803 (2006).
[13] J. T. Liu, Phys. Rev. D **50**, 542 (1994).
[14] D. Ng, Phys. Rev. D **49**, 4805 (1994).
[15] R. Foot, H. N. Long, and T. A. Tran, Phys. Rev. D **50**, R34 (1994); H. N. Long, Phys. Rev. D **53**, 437 (1996); **54**, 4691 (1996).
[16] J. C. Montero, F. Pisano, and V. Pleitez, Phys. Rev. D **47**, 2918 (1993).
[17] H. N. Long and V. T. Van, J. Phys. G **25**, 2319 (1999).
[18] D. A. Gutierrez, W. A. Ponce, and L. A. Sanchez, Eur. Phys. J. C **46**, 497 (2006).
[19] R. A. Diaz, R. Martinez, and F. Ochoa, Phys. Rev. D **72**, 035018 (2005); F. Ochoa and R. Martinez, Phys. Rev. D **72**, 035010 (2005); arXiv:hep-ph/0508082; A. Carcamo,

R. Martinez, and F. Ochoa, Phys. Rev. D **73**, 035007 (2006).
[20] Y. Okamoto and M. Yasue, Phys. Lett. B **466**, 267 (1999).
[21] T. Kitabayashi and M. Yasue, Phys. Rev. D **63**, 095002 (2001).
[22] M. B. Tully and G. C. Joshi, Phys. Rev. D **64**, 011301 (2001).
[23] J. C. Montero, C. A. De S. Pires, and V. Pleitez, Phys. Rev. D **65**, 095001 (2002).
[24] N. V. Cortez and M. D. Tonasse, Phys. Rev. D **72**, 073005 (2005).
[25] T. V. Duong and E. Ma, Phys. Lett. B **316**, 307 (1993).
[26] J. C. Montero, V. Pleitez, and M. C. Rodriguez, Phys. Rev. D **65**, 035006 (2002).
[27] J. C. Montero, V. Pleitez, and M. C. Rodriguez, Phys. Rev. D **70**, 075004 (2004).
[28] W. A. Ponce, Y. Giraldo, and L. A. Sanchez, Phys. Rev. D **67**, 075001 (2003); P. V. Dong, H. N. Long, D. T. Nhung, and D. V. Soa, Phys. Rev. D **73**, 035004 (2006).
[29] N. T. Anh, N. A. Ky, and H. N. Long, Int. J. Mod. Phys. A **16**, 541 (2001).
[30] R. A. Diaz, R. Martinez, and F. Ochoa, Phys. Rev. D **69**, 095009 (2004).
[31] A. G. Dias, R. Martinez, and V. Pleitez, Eur. Phys. J. C **39**, 101 (2005).
[32] U. Haisch, arXiv:0706.2056.
[33] M. Misiak *et al.*, Phys. Rev. Lett. **98**, 022002 (2007).
[34] K. Bieri, C. Greub, and M. Steinhauser, Phys. Rev. D **67**, 114019 (2003); M. Misiak and M. Steinhauser, Nucl. Phys. **B683**, 277 (2004); M. Gorbahn and U. Haisch, Nucl. Phys. **B713**, 291 (2005); M. Gorbahn, U. Haisch, and M. Misiak, Phys. Rev. Lett. **95**, 102004 (2005); K. Melnikov and A. Mitov, Phys. Lett. B **620**, 69 (2005); I. Blokland, A. Czarnecki, M. Misiak, M. Slusarczyk, and F. Tkachov, Phys. Rev. D **72**, 033014 (2005); H. M. Asatrian, A. Hovhannisyan, V. Poghosyan,

T. Ewerth, C. Greub, and T. Hurth, Nucl. Phys. **B749**, 325 (2006); H. M. Asatrian, T. Ewerth, A. Ferroglia, P. Gambino, and C. Greub, Nucl. Phys. **B762**, 212 (2007); M. Czakon, U. Haisch, and M. Misiak, J. High Energy Phys. 03 (2007) 008; M. Misiak and M. Steinhauser, Nucl. Phys. **B764**, 62 (2007).

[35] The Heavy Flavor Averaging Group (HFAG), http://www.slac.stanford.edu/xorg/hfag/.

[36] M. Ciuchini, G. Degrassi, P. Gambino, and G. F. Giudice, Nucl. Phys. **B527**, 21 (1998); F. Borzumati and C. Greub, Phys. Rev. D **58**, 074004 (1998).

[37] M. Ciuchini, G. Degrassi, P. Gambino, and G. F. Giudice, Nucl. Phys. **B534**, 3 (1998); F. Borzumati, C. Greub, and Y. Yamada, Phys. Rev. D **69**, 055005 (2004); G. Degrassi, P. Gambino, and P. Slavich, Phys. Lett. B **635**, 335 (2006); G. Degrassi, P. Gambino, and G. F. Giudice, J. High Energy Phys. 12 (2000) 009; M. S. Carena, D. Garcia, U. Nierste, and C. E. M. Wagner, Phys. Lett. B **499**, 141 (2001); A. J. Buras, P. H. Chankowski, J. Rosiek, and L. Slawianowska, Nucl. Phys. **B659**, 3 (2003); A. Freitas, E. Gasser, and U. Haisch, Phys. Rev. D **76**, 014016 (2007); G. D'Ambrosio, G. F. Giudice, G. Isidori, and A. Strumia, Nucl. Phys. **B645**, 155 (2002); F. Borzumati, C. Greub, T. Hurth, and D. Wyler, Phys. Rev. D **62**, 075005 (2000); T.

Besmer, C. Greub, and T. Hurth, Nucl. Phys. **B609**, 359 (2001); M. Ciuchini, E. Franco, A. Masiero, and L. Silvestrini, Phys. Rev. D **67**, 075016 (2003); **68**, 079901 (E) (2003); J. Foster, K. i. Okumura, and L. Roszkowski, J. High Energy Phys. 08 (2005) 094; **641**, 452 (2006); M. Ciuchini, A. Masiero, P. Paradisi, L. Silvestrini, S. K. Vempati, and O. Vives, Nucl. Phys. **B783**, 112 (2007).

[38] K. Agashe, N. G. Deshpande, and G. H. Wu, Phys. Lett. B **514**, 309 (2001); A. J. Buras, A. Poschenrieder, M. Spranger, and A. Weiler, Nucl. Phys. **B678**, 455 (2004); U. Haisch and A. Weiler, Phys. Rev. D **76**, 034014 (2007).

[39] A. Freitas and U. Haisch, Phys. Rev. D **77**, 093008 (2008).

[40] M. Blanke, A. J. Buras, A. Poschenrieder, C. Tarantino, S. Uhlig, and A. Weiler, J. High Energy Phys. 12 (2006) 003; M. Blanke, A. J. Buras, S. Recksiegel, C. Tarantino, and S. Uhlig, J. High Energy Phys. 06 (2007) 082.

[41] W. j. Huo and S. h. Zhu, Phys. Rev. D **68**, 097301 (2003); A. J. Buras, A. Poschenrieder, S. Uhlig, and W. A. Bardeen, J. High Energy Phys. 11 (2006) 062.

[42] M. Misiak and M. Steinhauser, Nucl. Phys. **B764**, 62 (2007).

[43] V. M. Abazov *et al.* (D0 Collaboration), Phys. Rev. D **76**, 057101 (2007).